THE JOURNAL OF BIOLOGICAL CHEMISTRY Vol. 279, No. 34, Issue of August 20, pp. 35557–35563, 2004
Printed in U.S.A.

Mechanism of Blebbistatin Inhibition of Myosin II*

Received for publication, May 12, 2004, and in revised form, June 14, 2004
Published, JBC Papers in Press, June 16, 2004, DOI 10.1074/jbc.M405319200

Mihály Kovács‡, Judit Tóth‡§, Csaba Hetényi§¶, András Málnási-Csizmadia§¶, and James R. Sellers‡‖

From the ‡Laboratory of Molecular Cardiology, NHLBI, National Institutes of Health, Bethesda, Maryland 20892-1762 and the §Department of Biochemistry, Eötvös University, Pázmány P. sétány 1-C, H-1117 Budapest, Hungary

Blebbistatin is a recently discovered small molecule inhibitor showing high affinity and selectivity toward myosin II. Here we report a detailed investigation of its mechanism of inhibition. Blebbistatin does not compete with nucleotide binding to the skeletal muscle myosin subfragment-1. The inhibitor preferentially binds to the ATPase intermediate with ADP and phosphate bound at the active site, and it slows down phosphate release. Blebbistatin interferes neither with binding of myosin to actin nor with ATP-induced actomyosin dissociation. Instead, it blocks the myosin heads in a products complex with low actin affinity. Blind docking molecular simulations indicate that the productive blebbistatin-binding site of the myosin head is within the aqueous cavity between the nucleotide pocket and the cleft of the actin-binding interface. The property that blebbistatin blocks myosin II in an actin-detached state makes the compound useful both in muscle physiology and in exploring the cellular function of cytoplasmic myosin II isoforms, whereas the stabilization of a specific myosin intermediate confers a great potential in structural studies.

Myosin IIs are ATP-driven molecular motors forming an essential part of the motile machinery of most eukaryotic cell types examined. Among other functions, they serve such diverse and vital functions as muscle contraction, cytokinesis, cortical tension maintenance, and neurite outgrowth and retraction (1–6). In studies of myosin II, the use of enzyme inhibitors can be a powerful approach, provided that selective and high affinity compounds are available that do not interfere with other cellular processes. The importance of the latter aspect is emphasized by a recent study (7) that showed that 2,3-butanedione-monoxime, a compound widely used to inhibit myosin II, is not specific and probably affects the function of a wide range of proteins.

Blebbistatin was recently discovered as a small molecule inhibitor of muscle and non-muscle myosin II (8). The compound is permeable to cell membranes. It is a potent inhibitor of skeletal muscle and non-muscle myosin II isoforms, although it has little or no effect on smooth muscle myosin II and myosins from classes I, V, and X (9). Because of its selectivity and high affinity for several class II myosins, blebbistatin has the potential to become a popular tool in the fields of cell motility and muscle physiology. For the interpretation of the cellular effects caused by blebbistatin, a detailed understanding is essential of its effects on the myosin II ATPase and on the interaction of the myosin head with actin and substrate. We undertook an in-depth characterization of the effect of blebbistatin on the functional properties of rabbit skeletal muscle myosin II, and we performed blind docking simulations on various atomic structures of the myosin head to determine the binding site and the structural basis of isoform specificity of the inhibitor.

We find that blebbistatin exerts its inhibitory effect by binding to the myosin-ADP-P_i complex with high affinity and interfering with the phosphate release process. Thus, the inhibitor blocks myosin in an actin-detached state, and therefore it prevents rigid actomyosin cross-linking, which is a great advantage in *in vivo* applications. By using molecular simulations, we identify the aqueous cavity between the nucleotide- and actin-binding sites of the myosin head as the productive binding site for blebbistatin. All myosin IIs characterized to date follow a common basic enzymatic mechanism (10). Therefore, the mode of inhibition of other muscle and non-muscle myosin II isoforms is expected to be similar to those described herein.

EXPERIMENTAL PROCEDURES

Materials—Rabbit fast skeletal muscle myosin and subfragment-1 (S1)[1] were prepared as described in Refs. 11 and 12, respectively. Actin was prepared as in Ref. 13 and pyrene-labeled as in Ref 14. Blebbistatin was either generously provided by Drs. Aaron F. Straight and Timothy J. Mitchison (Harvard Medical School) or purchased from Toronto Research Chemicals. Contrasting with previous observations (8), we found that the $K_{½}$ values and maximal extents of inhibition by the two stereoisomers of blebbistatin are very similar (data not shown). Therefore, we used an unresolved blebbistatin mixture in all experiments.

Conditions—If not stated otherwise, experiments were carried out at 25 °C. For experiments not involving actin plus those in Fig. 5, the following assay buffer was used: 20 mM MOPS (pH 7.0), 5 mM $MgCl_2$, 100 mM KCl, 0.1 mM EGTA. For experiments involving actin except those in Fig. 5, the following assay buffer was used: 4 mM MOPS (pH 7.0), 2 mM $MgCl_2$, 0.1 mM EGTA. Mg^{2+} concentration was always kept higher than total nucleotide concentration.

Steady-state ATPase Assay—MgATPase activities were measured by an NADH-linked assay as described previously (15) in 1 mM ATP. Data were corrected for background ATPase activity of actin.

Stopped-flow Experiments—These experiments were carried out in a KinTek SF-2001 instrument. Fluorescence excitation/emission setups were the following: tryptophan, 295/347-nm bandpass (50 nm bandwidth); mant and pyrene, 365 nm/400 nm long pass. Light scattering was measured at 340 nm. Actin filaments were stabilized by addition of a 1.5-fold molar excess of phalloidin. If not stated otherwise, post-mixing concentrations are as indicated throughout the text. Exceptions are the stopped-flow-based equilibrium titrations, where preincubation concentrations are relevant in the analysis of signal change amplitudes,

* This work was funded by the EMBO/HHMI Young Investigator Programme and the Wellcome Trust (to A. M. C.). The costs of publication of this article were defrayed in part by the payment of page charges. This article must therefore be hereby marked "*advertisement*" in accordance with 18 U.S.C. Section 1734 solely to indicate this fact.

¶ Békésy Fellow of the Hungarian Ministry of Education.

‖ To whom correspondence should be addressed: Laboratory of Molecular Cardiology, NHLBI, National Institutes of Health, Bldg. 10, Rm. 8N202, Bethesda, MD 20892-1762. Tel.: 301-496-6887; Fax: 301-402-1542; E-mail: sellersj@nhlbi.nih.gov.

[1] The abbreviations used are: S1, subfragment-1; mant, 2′(3)-*O*-(*N*-methylanthraniloyl); MOPS, 4-morpholinepropanesulfonic acid.

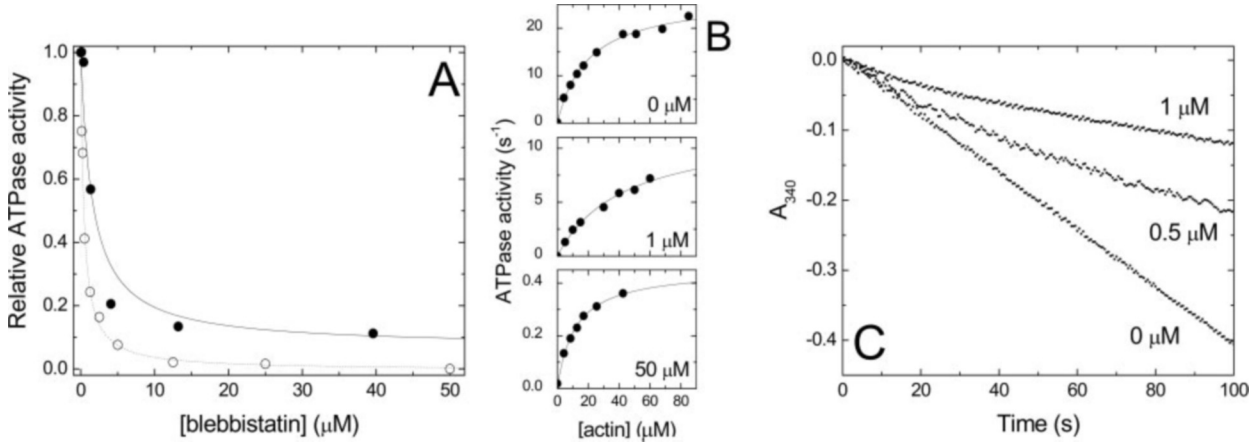

FIG. 1. **Inhibition of the steady-state ATPase activity of S1 by blebbistatin.** *A*, relative basal (*solid circles*) and actin-activated (*open circles*) steady-state ATPase activities of S1 at different blebbistatin concentrations. The basal ATPase activity (0.08 s^{-1}) was inhibited to a maximal extent of 91% ($K_{½}$ = 1.4 μM), whereas the actin-activated ATPase activity (18 s^{-1} at 43 μM actin) was almost totally inhibited (by 99%) with a $K_{½}$ of 0.4 μM in the experiments shown. *B*, actin activation of S1 ATPase at the indicated blebbistatin concentrations. V_{max} and K_{ATPase} values were 26 s^{-1} and 24 μM (0 μM blebbistatin), 12 s^{-1} and 43 μM (1 μM blebbistatin), and 0.45 s^{-1} and 11 μM (50 μM blebbistatin), respectively. *C*, onset of the inhibition of S1 ATPase activity on mixing 30 nM S1, 50 μM actin, and blebbistatin at the indicated concentrations with 1 mM ATP. Measured absorbance values were corrected to the start point of the reaction. Measurements were performed by using an NADH-linked enzyme assay as described (15). The conditions were as follows: 25 °C, 4 mM MOPS (pH 7.0), 2 mM $MgCl_2$, 0.1 mM EGTA.

whereas the k_{obs} values will reflect post-mix concentrations. Volume ratios in stopped-flow mixtures were 1:1 in all experiments.

Quenched-flow Experiments—These experiments were performed in a KinTek RQF-3 apparatus by using [γ-^{32}P]ATP as described earlier (15). Reagent concentrations after mixing are indicated.

Acto-S1 Cosedimentation—50–100-μl samples were ultracentrifuged at 100,000 rpm in a Beckman TLA-100 rotor for 15 min at 4 °C, and the supernatants and pellets were analyzed by 4–20% SDS-PAGE. Relative amounts of proteins in electrophoretic bands were determined by densitometry using the Kodak ID 3.5 software.

Data Analysis—Reported means and standard errors are those of two to six rounds of experiment. Fitting of the data sets was done using the KinTek software and OriginLab 7.0 (Microcal Corp.).

Computational Docking—Throughout the search for putative binding sites of (*R*)-(+)- and (*S*)-(−)-blebbistatin on the myosin head was performed by using our previously published blind docking approach (16) with the AutoDock 3.0 program package (17). Atomic structures for head domains of nucleotide-free skeletal muscle myosin (2MYS), ADP·BeF_x-bound smooth muscle myosin (1BR4), *Dictyostelium* myosin II with ATP (1FMW) or ADP·AlF_4 (1MND) bound, and nucleotide-free myosin V (1OE9) of the Protein Data Bank were applied as target molecules during the calculations. For each protein and enantiomer of blebbistatin, 100 docking runs were evaluated. Representative groups (*i.e.* the binding patterns) were collected and ordered based on the calculated binding free energy of the complexes (16).

RESULTS

Steady-state Inhibition—In the experiments described, we used a soluble head fragment of skeletal myosin (S1) that contains the actin- and nucleotide-binding sites and retains the enzymatic properties of the full-length molecule (10). "S1" refers to rabbit skeletal muscle S1 throughout this article. The basal MgATPase activity of S1 measured in the absence of actin (0.08 ± 0.01 s^{-1} in the absence of blebbistatin) was inhibited by blebbistatin to a large extent (92 ± 4% maximal inhibition) with half-maximal inhibition at 1.6 ± 0.6 μM blebbistatin (Fig. 1*A*, see also Table I for a summary of parameters determined in this study). The acto-S1 ATPase activity (uninhibited V_{max} = 24.0 ± 1.5 s^{-1}) was almost totally inhibited with half-maximal inhibition at 0.4 ± 0.1 μM blebbistatin (Fig. 1*A*). Nevertheless, actin activated the low inhibited basal S1 ATPase (0.005 ± 0.001 s^{-1}) even in 50 μM blebbistatin to a maximum of 0.45 ± 0.02 s^{-1} (about 2% of the uninhibited activity) (Fig. 1*B*). The inhibitor did not have a systematic effect on the K_{ATPase} value (*i.e.* the actin concentration at half-maximal activation, Fig. 1*B* and Table I).

At low blebbistatin concentrations where the binding equilibrium between enzyme and inhibitor is slow compared with enzymatic turnover, an initial nonlinear phase in activity could be observed whereby the system was reaching steady-state inhibition. Fig. 1*C* shows that at low blebbistatin concentrations, the onset of the blebbistatin-inhibited steady-state of the acto-S1 ATPase was preceded by a slow exponential phase whose observed rate constant (k_{obs}) fell between 0.02 and 0.07 s^{-1} in the blebbistatin concentration range of 0.5–4 μM, and indicated that the blebbistatin off-rate constant from S1 during ATP turnover is below 0.02 s^{-1} and the on-rate constant is in the order of 0.01 μM^{-1} s^{-1} (data not shown). These values define a K_d value of blebbistatin binding to S1 around 1 μM, close to the above half-maximal inhibition value. The precise dependence of k_{obs} on blebbistatin concentration could not be reliably determined because the rate constants of the exponential and linear phases were highly covariant. It is noteworthy that in these experiments several hundred ATP turnovers had occurred before the system reached steady-state inhibition (the uninhibited acto-S1 ATPase activity was 20 s^{-1} under the conditions used).

Blebbistatin Binding to S1 ATPase Intermediates—The conformational changes of the myosin head occurring during ATP binding, hydrolysis, and product release cause changes in its tryptophan fluorescence that have been extensively utilized to monitor the ATPase cycle (18–26). When S1 was mixed with excess ATP in the absence of blebbistatin, an initial rapid increase in S1 tryptophan fluorescence that reflects the binding of ATP was followed by a steady state with a constantly elevated fluorescence level (Fig. 2*A*). When the ATP solution also contained blebbistatin, the initial fluorescence increase was followed by a quench phase leading to a steady-state fluorescence level that is 5–10% lower than that of apoS1 (Fig. 2*A*). The quench phase was a single exponential, and its k_{obs} was linearly dependent on blebbistatin concentration with a slope of 0.0034 ± 0.0002 μM^{-1} s^{-1} (reflecting the on-rate constant of blebbistatin binding to S1 during steady-state ATP hydrolysis, Table I) and an intercept of 0.011 ± 0.003 s^{-1} (off-rate, Fig. 2*B*).

A fluorescent S1 substrate, mant-ATP, shows a fluorescence increase on binding to S1. When S1 was mixed with excess mant-ATP in the stopped flow, an initial fluorescence increase was followed by a period with high mant fluorescence (Fig. 2*C*). When 50 μM blebbistatin was included in both syringes, the initial increase was followed by a quench phase whose k_{obs}

($0.21\ s^{-1}$) was similar to that of the tryptophan fluorescence quench at the same blebbistatin concentration (*cf.* Fig. 2, *A* and *C*, note the different time scales of the two panels). The results in Fig. 2 suggest that blebbistatin will bind to a nucleotide-bound S1 ATPase intermediate slowly but with high affinity (K_d = 3.1 ± 0.8 μM, close to the concentration needed for half-maximal steady-state inhibition, *cf.* Table I), and its binding is accompanied by a quench in both tryptophan and mant fluorescence.

TABLE I
Effect of blebbistatin on skeletal muscle S1 ATPase
Nomenclature of steps refers to Scheme 1 where applicable.

	−Blebbistatin	+Blebbistatin[a]
Basal ATPase[b]		
Activity (s^{-1})	0.08 ± 0.01	0.006 ± 0.003
$K_{½}$ for blebbistatin (μM)		1.6 ± 0.6
Maximal inhibition (%)		92 ± 4
Actin-activated ATPase[b]		
V_{max} (s^{-1})	24.0 ± 1.5	0.45 ± 0.02
K_{ATPase} (μM)	24 ± 4	11 ± 2
$K_{½}$ for blebbistatin (μM)		0.4 ± 0.1
Maximal inhibition (%)		98 ± 2
Actin-bound fraction of S1 in ATP (50 μM actin)[c]	0.1	0.04
ATP interaction		
k_1 ($\mu M^{-1}\ s^{-1}$)[d]	2.0 ± 0.3	1.2 ± 0.2
$k_2 + k_{-2}$ (s^{-1})[d]	135 ± 15	95 ± 2
P_i burst amplitude (mol/mol)[e]	0.26 ± 0.04	0.80 ± 0.13
K_2[f]	0.35	4
ADP interaction		
k_4 (s^{-1})[d]	1.7 ± 0.2	1.1 ± 0.2
k_{-4} ($\mu M^{-1}\ s^{-1}$)[d]	1.4 ± 0.2	0.53 ± 0.07
K_4 (μM, k_4/k_{-4})	1.1 ± 0.4	2.1 ± 0.5
K_4 (μM, titration)[d]	1.41 ± 0.06	1.36 ± 0.11
Phosphate release		
k_3 (s^{-1})	0.08	≤0.005
Actin interaction[f]		
k_{on} ($\mu M^{-1}\ s^{-1}$)	4.7 ± 0.8	3.0 ± 0.5
K_d (μM, no nucleotide)	<0.05	<0.05
ATP-induced acto-S1 dissociation ($\mu M^{-1}\ s^{-1}$)	5.4 ± 0.1	4.8 ± 0.3
Blebbistatin binding to S1		
k_{MDP} (s^{-1})[d]		0.011 ± 0.003
k_{-MDP} ($\mu M^{-1}\ s^{-1}$)[d]		0.0034 ± 0.0002
K_{MDP} (μM)[d]		3.1 ± 0.8
K_{apo} (μM)[d]		25 ± 2
K_{MD} (μM)		24
K_{MT} (μM)		35
K_d(acto-S1) (μM)[c]		>100

[a] 50 μM unless indicated otherwise.
[b] NADH-linked assay.
[c] Acto-S1 cosedimentation.
[d] Tryptophan fluorescence.
[e] Quenched-flow.
[f] Pyrene-actin fluorescence.

The affinity of blebbistatin to apoS1 is also of interest. Blebbistatin itself is luminescent, but neither the inhibitor nor S1 showed an analyzable signal change on mixing the two components. When preincubated with S1, however, blebbistatin caused a detectable decrease in the apparent ATP binding rate constant of S1 (Table I). Considering that ATP binding is a fast process, this effect is likely caused by a pre-existing interaction between S1 and the inhibitor. We determined the affinity of blebbistatin for apoS1 by an indirect experiment analyzing the tryptophan fluorescence transients on rapidly mixing ATP with S1 preincubated with different concentrations of blebbistatin. In the absence of blebbistatin, a single exponential increase with a k_{obs} of 85 s^{-1} was observed at 100 μM (pre-mix) ATP concentration (Fig. 3*A*). When S1 was preincubated with blebbistatin, double exponential traces were obtained with phases around 85 and 30 s^{-1}. The fractional amplitude of the slow phase ($A_{slow}/(A_{fast} + A_{slow})$) increased with increasing blebbistatin concentration, and the obtained trace was essentially a single exponential with a k_{obs} around 30 s^{-1} above 100 μM (pre-mix) blebbistatin (Fig. 3*B*). Even though the two k_{obs} values of the biphasic traces were separated only by about a factor of 3, the fractional amplitude of the slow phase plotted against blebbistatin concentration fitted well to a hyperbola and showed a K_d of 25 ± 2 μM for blebbistatin binding to apoS1 (Fig. 3*B*).

The ADP affinity of S1 was measured by preincubating 0.2 μM S1 with various amounts of ADP in the absence and presence of 100 μM blebbistatin and then rapidly mixing with 100 μM ATP (pre-mix concentrations stated, traces not shown). The slow phase (k_{obs} = 1.7 ± 0.2 s^{-1} in the absence and 1.1 ± 0.2 s^{-1} in the presence of blebbistatin) of the obtained biphasic tryptophan fluorescence increase transients represents the fraction of S1 that was ADP-bound before the rapid mix. Here ADP dissociation limits the rate of ATP binding and therefore that of the fluorescence change. The fast phase (k_{obs} = 70 s^{-1} in the absence and 30 s^{-1} in the presence of 100 μM (pre-mix) blebbistatin) represents the S1 fraction that did not contain bound nucleotide and thus could directly bind ATP. The fractional amplitude of the slow phase showed a hyperbolic dependence on ADP concentration, and very similar K_d values were determined in the absence and presence of blebbistatin (1.41 ± 0.06 and 1.36 ± 0.11 μM, respectively, Fig. 3*C*). The ADP

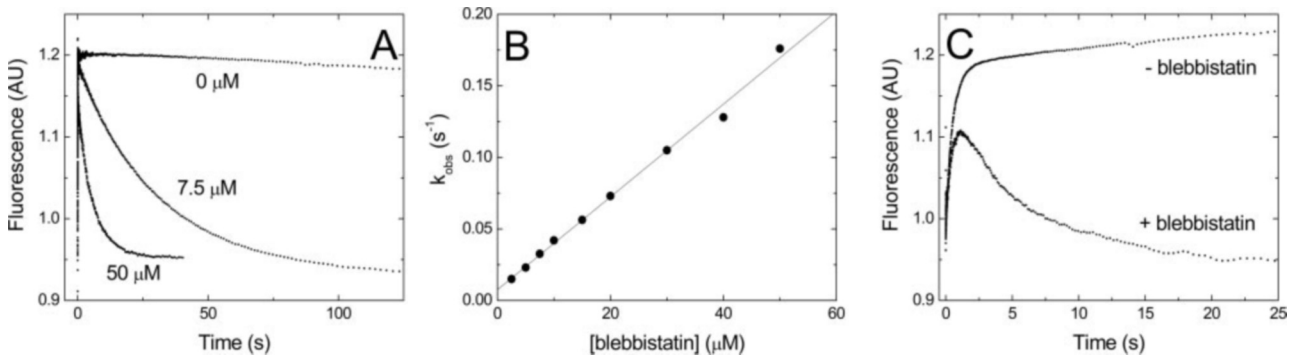

FIG. 2. **Blebbistatin binding to S1 during basal ATP turnover.** *A*, tryptophan fluorescence transients recorded on mixing 0.5 μM S1 with 50 μM ATP plus blebbistatin at the indicated concentrations. In the presence of blebbistatin, the initial rapid fluorescence increase was followed by a quench phase (k_{obs} = 0.03 s^{-1} at 7.5 μM blebbistatin and 0.18 s^{-1} at 50 μM blebbistatin) leading to a fluorescence level that is 5–10% lower than that of apoS1. Traces were normalized to their starting values. *B*, dependence of k_{obs} of the quench phase on blebbistatin concentration. Linear fit to the data yielded a slope of 0.0033 $\mu M^{-1}\ s^{-1}$ and an intercept of 0.0076 s^{-1} in the experiment shown. *C*, mant-ATP fluorescence transients on mixing 0.1 μM S1 with 0.5 μM mant-ATP in the absence and presence of 50 μM blebbistatin (in all syringes). Without blebbistatin, an initial fluorescence increase (k_{obs} = 2.1 s^{-1}) was followed by a period with elevated mant fluorescence. In blebbistatin, the initial increase (k_{obs} = 2.1 s^{-1}) was followed by a quench with a k_{obs} of 0.21 s^{-1}. Traces were normalized to their starting values. The conditions are as follows: 25 °C, 20 mM MOPS (pH7.0), 5 mM $MgCl_2$, 100 mM KCl, 0.1 mM EGTA. *AU*, arbitrary units.

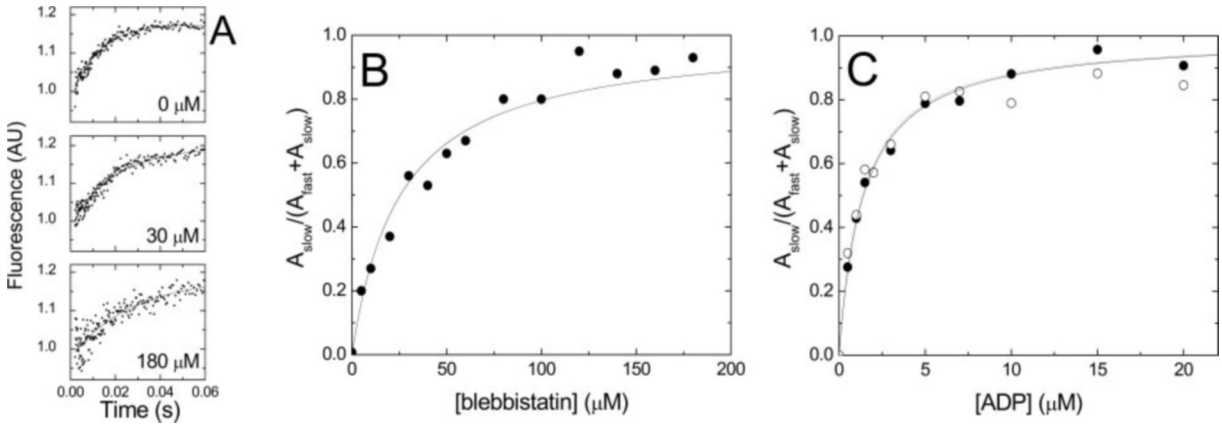

FIG. 3. **Interaction of blebbistatin with apoS1 and S1·ADP.** *A*, tryptophan fluorescence transients on mixing 0.5 μM S1 plus blebbistatin at the indicated concentrations with 100 μM ATP (pre-mixing concentrations stated). The k_{obs} values were 85 s^{-1} (0 μM blebbistatin) and 30 s^{-1} (180 μM blebbistatin). At 30 μM blebbistatin, the trace was a double exponential with phases around 85 and 30 s^{-1}. Traces were normalized to their starting values. *B*, fractional amplitude of the slow (30 s^{-1}) phase ($A_{slow}/(A_{fast} + A_{slow})$) as a function of blebbistatin concentration. Hyperbolic fit to the data yielded a K_d of 25 ± 2 μM for blebbistatin binding to apoS1. *C*, 0.2 μM S1 plus ADP at different concentrations was preincubated in the absence (*solid circles*) and presence (*open circles*) of 100 μM blebbistatin and then rapidly mixed with 100 μM ATP (pre-mix concentrations stated). Fractional amplitude of the slow phase ($A_{slow}/(A_{fast} + A_{slow})$) of the obtained biphasic tryptophan fluorescence transients is plotted against ADP concentration. From hyperbolic fits to the data, K_d values for ADP binding to S1 were 1.41 ± 0.06 μM in the absence and 1.36 ± 0.11 μM in the presence of 100 μM blebbistatin. Observed rate constants of the traces were 66 ± 14 s^{-1} and 1.7 ± 0.2 s^{-1} in the absence and 28 ± 7 s^{-1} and 1.1 ± 0.2 s^{-1} in the presence of blebbistatin. The conditions were as in Fig. 2. Pre-mixing concentrations are stated throughout this figure. *AU*, arbitrary units.

affinity of S1 in the absence and presence of blebbistatin was also assessed in a similar stopped-flow titration where 0.1 μM S1 was preincubated with various ADP concentrations and then rapidly mixed with 20 μM mant-ATP, and the fluorescence signal of the mant nucleotide was monitored. Similarly to the tryptophan experiments, biphasic fluorescence traces were obtained yielding a K_d of S1 for ADP of 1.04 ± 0.03 μM in the absence and 0.77 ± 0.03 μM in the presence of 50 μM blebbistatin (plot not shown).

Effect of Blebbistatin on ATP Hydrolysis—To observe directly the effect of blebbistatin on the ATP hydrolysis step, we performed quenched-flow experiments using ATP radioactively labeled on its γ-phosphate. When 5 μM S1 was mixed with a 10-fold excess of ATP, an initial rapid exponential burst (k_{obs} = 40 s^{-1}) in P_i production was observed that was followed by a linear steady-state phase (Fig. 4*A*). The slope of the steady-state phase (0.06 ± 0.01 s^{-1}) was consistent with the basal ATPase activity of S1 measured by the steady-state assay (Table I). The amplitude of the burst was 0.26 ± 0.04 mol of P_i/mol of S1. In the presence of 50 μM blebbistatin (in all syringes), the burst phase (k_{obs} = 20 s^{-1}) amplitude was elevated to 0.80 ± 0.13 mol of P_i/mol of S1, whereas the linear steady-state phase was inhibited by ~80% (Fig. 4*A*). In single turnover quenched-flow experiments, 2.5 μM S1 was mixed with 1 μM ATP in the absence and presence of 50 μM blebbistatin (in all syringes) (Fig. 4*B*). Here the kinetics of the fast phase of ATP hydrolysis is limited by nucleotide binding, whereas the slow phase reflects P_i release. Double exponential approximations to the time courses showed similar burst values to the multiple turnover experiments.

Because the ATP hydrolysis step is followed by the rate-limiting release of phosphate, the amplitude of the initial burst (expressed as n_{P_i}/n_{S1} in multiple turnover, and the fractional amplitude of the fast phase in the single turnover experimental setup) will define the equilibrium constant of the ATP hydrolysis step on the enzyme as $K = A/(1 - A)$, where A is the P_i burst amplitude. The obtained burst amplitude and hydrolysis equilibrium constant in the absence of blebbistatin was considerably lower than the literature values available (27), which likely reflects the pH dependence of this reaction step (our measurements were performed at pH 7, whereas earlier experiments were done at pH 8). The amplitude was well reproducible in our experiments. The reported data are from six independent experiments performed on three different S1 preparations. Data obtained with freshly prepared and previously fast-frozen material were identical. All other kinetic parameters determined with our S1 preparations were in line with literature values.

Effect of Blebbistatin on the Actin Interaction of S1—The quench in pyrene fluorescence that occurs on pyrene-actin binding to S1 was used to follow the actin binding kinetics of S1. As shown in Fig. 5*A*, the presence of 50 μM blebbistatin does not cause a profound change in the acto-S1 binding rate constant (k_{on} = 4.7 ± 0.8 μM^{-1} s^{-1} in the absence and 3.0 ± 0.5 μM^{-1} s^{-1} in the presence of 50 μM blebbistatin in all syringes). The rigor actin binding affinity (*i.e.* that in the absence of nucleotides) of S1 was investigated by a stopped-flow-based titration where 0.1 μM pyrene-actin was preincubated with various amounts of S1 and then rapidly mixed with excess ATP to fully dissociate acto-S1. Thus, the total amplitudes of the recorded pyrene fluorescence transients reflect the concentration of the strongly actin-bound fraction of S1 before mixing with ATP. Quadratic fits of the dependence of the observed amplitudes on S1 concentration (28) showed that the presence of 50 μM blebbistatin (in all syringes) had no detectable effect on the observed actin affinity of S1 (K_d < 50 nM, Fig. 5*B*).

The kinetics of ATP-induced acto-S1 dissociation was measured by monitoring the pyrene fluorescence increase on mixing pyrene-acto-S1 with increasing concentrations of ATP. Fig. 5*C* shows that the presence of 50 μM blebbistatin (in all syringes) did not significantly change the apparent second order binding constant of ATP to acto-S1 (5.4 ± 0.1 μM^{-1} s^{-1} in the absence and 4.8 ± 0.3 μM^{-1} s^{-1} in the presence of 50 μM blebbistatin in all syringes; Table I).

The lack of effect of the presence of blebbistatin in the experiments of Fig. 5, *B* and *C*, indicates that either the actin-related properties of blebbistatin-bound S1 are unchanged compared with blebbistatin-free S1 or, more probably, that acto-S1 has a very low blebbistatin affinity, and little of the acto-S1 complexes has bound blebbistatin (see below).

Distribution of Actin-bound and Detached S1 States during Steady-state ATP Hydrolysis—In light scattering and pyrene-

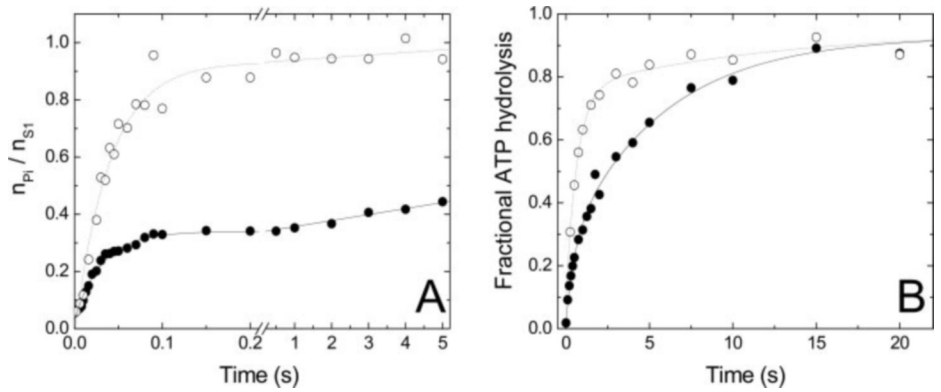

FIG. 4. **Effect of blebbistatin on the ATP hydrolysis step.** *A*, time courses of ATP hydrolysis on mixing 5 μM S1 with 50 μM ATP in the absence (*solid circles*) and presence (*open circles*) of 50 μM blebbistatin (in all syringes) in the quenched-flow apparatus. The single exponential P_i burst (k_{obs} = 40 s^{-1} in the absence and 20 s^{-1} in the presence of blebbistatin) was followed by a linear steady-state phase. The amplitude of the burst calculated as $n_{P_i(burst)}/n_{S1(total)}$ was 0.31 in the absence and 0.90 in the presence of blebbistatin in the experiments shown. Note the break in the *x* axis. *B*, single turnover experiment in which 1 μM ATP was mixed with 2.5 μM S1 in the absence (*solid symbols*) and presence (*open symbols*) of 50 μM blebbistatin. Double exponential approximations to the time courses of the reactions are shown. The initial P_i burst of the reaction as determined from the amplitudes of the two phases as $A_{fast}/(A_{fast} + A_{slow})$ was 0.26 in the absence and 0.76 in the presence of blebbistatin in the experiments shown. Conditions were as in Fig. 2.

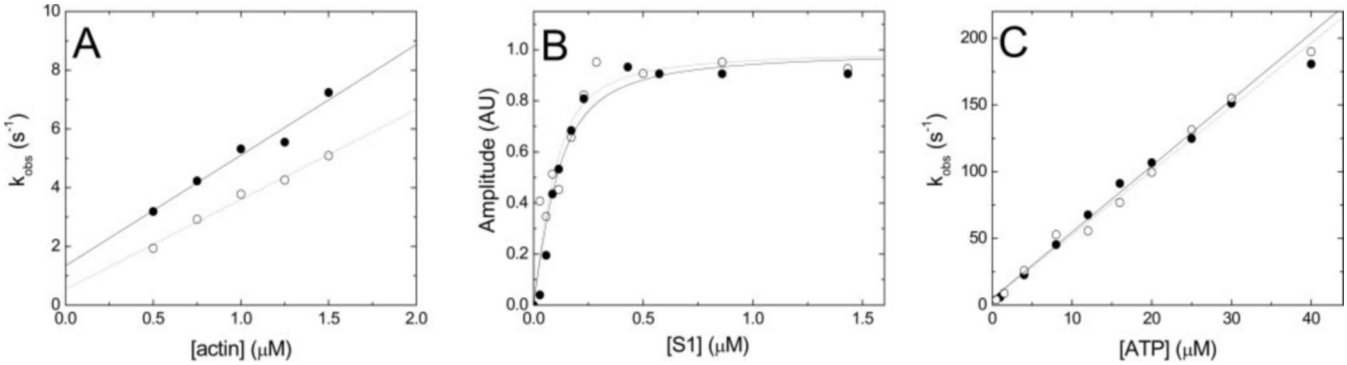

FIG. 5. **Effect of blebbistatin on actin binding of S1 and ATP-induced acto-S1 dissociation.** *A*, dependence of k_{obs} of the observed pyrene fluorescence quench on mixing 0.1 μM S1 with pyrene-actin at concentrations indicated in the absence (*solid symbols*) and presence (*open symbols*) of 50 μM blebbistatin (in all syringes). In the experiments shown, linear fits revealed on-rate constants of 3.7 and 3.3 μM^{-1} s^{-1} in the absence and presence of blebbistatin, respectively. *B*, binding curves of S1 to actin. 0.1 μM pyrene-actin was preincubated with various concentrations of S1 and rapidly mixed with 40 μM ATP (pre-mixing concentrations) in the absence (*solid symbols*) and presence (*open symbols*) of 50 μM blebbistatin (in all syringes). Amplitudes of the resulting pyrene fluorescence increase are shown normalized to their fitted maximal values. Quadratic fits yielded a K_d of 0.055 ± 0.017 μM in the absence and 0.040 ± 0.020 μM in the presence of blebbistatin. *C*, k_{obs} of ATP-induced acto-S1 dissociation on mixing 0.2 μM S1 and 0.1 μM pyrene-actin with ATP at the indicated concentrations in the absence (*solid symbols*) and presence (*open symbols*) of 50 μM blebbistatin (in all syringes). The apparent ATP binding rate constant of acto-S1 was 5.4 μM^{-1} s^{-1} in the absence and 4.8 μM^{-1} s^{-1} in the presence of blebbistatin in the data set shown. Conditions were as in Fig. 2. *AU*, arbitrary units.

actin fluorescence measurements performed by mixing 2 μM S1 plus 5 μM actin with 20 μM ATP in the absence of blebbistatin, the rapid dissociation of acto-S1 (k_{obs} = 80 s^{-1}) was followed by a steady state with a constant signal level that lasted for about 10 s (a period expected for a 10-fold excess of substrate over S1 (Fig. 6*A*)), followed by a reversal of the initial signal change as all S1 rebound to actin when ATP was depleted. The pyrene fluorescence and light scattering changes had opposite signs, consistent with the fact that acto-S1 dissociation causes an increase in pyrene fluorescence and a decrease in light scattering. In the presence of 50 μM blebbistatin (in all syringes), the dissociation kinetics was similar (k_{obs} = 90 s^{-1}), but no restoration of the signal was observed in 60 s (Fig. 6*B*). This result implies that in blebbistatin, S1 is predominantly not strongly bound to actin during steady-state ATP hydrolysis, similarly to the case when the inhibitor is not present. Steady-state ATP hydrolysis was presumably not completed in the observed period in the presence of blebbistatin (*cf.* Fig. 1*A* and Table I).

In ultracentrifugation experiments, S1 alone (20 μM) was found entirely in the supernatants of the samples, whereas it fully cosedimented with 50 μM actin in the absence of nucleotide (Fig. 6*C*). Addition of 50 μM blebbistatin did not have an effect on these properties. After addition of 10 mM ATP to acto-S1, most of the S1 was found in the supernatants both in the absence and presence of blebbistatin, showing that the inhibitor does not dramatically alter the distribution of actin-bound and detached S1 states during steady-state ATP hydrolysis. Notably, in the presence of blebbistatin, a slightly smaller fraction of S1 was pelleted (Fig. 6*C* and Table I). As measured spectrophotometrically (blebbistatin has an absorbance peak at 422 nm) (8), practically all the blebbistatin was in the supernatants of all samples, indicating that actin-bound S1 did not detectably bind blebbistatin (data not shown).

Blind Docking of Blebbistatin on the Myosin Head—We performed blind docking simulations of blebbistatin enantiomers on various myosin atomic structures (skeletal muscle myosin, smooth muscle myosin, *Dictyostelium* myosin II in the open and closed conformations, and myosin V) to elucidate the structural basis of the interaction of S1 with blebbistatin. Computational mapping of the binding sites yielded interaction patterns for each blebbistatin-myosin complex. Binding patterns were compared based on experimentally determined $K_{½}$ values (9). Skeletal muscle myosin and *Dictyostelium* myosin II are strongly inhibited (half-maximal inhibition at 0.5 and 4.9 μM blebbistatin, respectively), whereas myosin V ($K_{½} > 150$ μM) and smooth muscle myosin ($K_{½}$ = 80 μM) are not or very poorly inhibited by

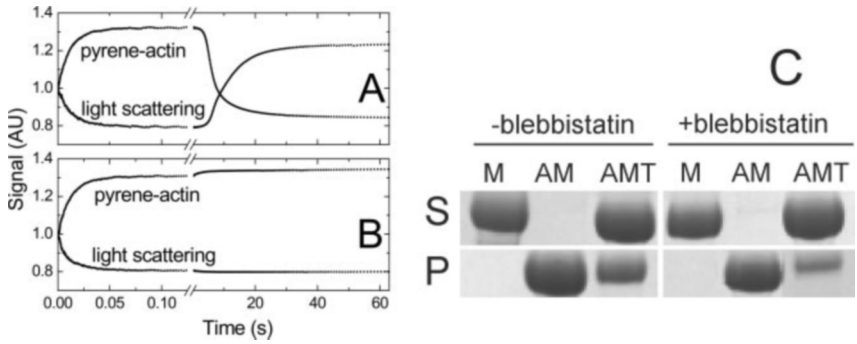

FIG. 6. **Effect of blebbistatin on the distribution of actin-bound and detached S1 states during ATP hydrolysis.** *A* and *B*, pyrene-actin fluorescence and light scattering transients on mixing a 5 μM pyrene-actin and 2 μM S1 with 20 μM ATP in the absence (*A*) and presence (*B*) of 50 μM blebbistatin (in all syringes). In the absence of blebbistatin, the rapid dissociation of acto-S1 (k_{obs} = 80 s^{-1}) was followed by an ~10-s period with a constant signal level before reversal of the initial signal changes. In blebbistatin, k_{obs} of the rapid phase was similar (90 s^{-1}), but no restoration of the signal was observed. Traces were normalized to their starting values. Note the break in the *x* axis. *C*, acto-S1 cosedimentation. The following samples (in the absence and presence of 50 μM blebbistatin) were analyzed by ultracentrifugation followed by SDS-PAGE: *M*, 20 μM S1; *AM*, 20 μM S1 + 50 μM actin; *AMT*, 20 μM S1 + 50 μM actin + 10 mM ATP. S1 heavy chain band of the supernatants (*S*) and pellets (*P*) is shown. In ATP, about 10 and 4% of S1 sedimented with actin in the absence and presence of blebbistatin, respectively. Spectrophotometric analysis showed that all blebbistatin was in the supernatant in all samples. Conditions were as in Fig. 1. *AU*, arbitrary units.

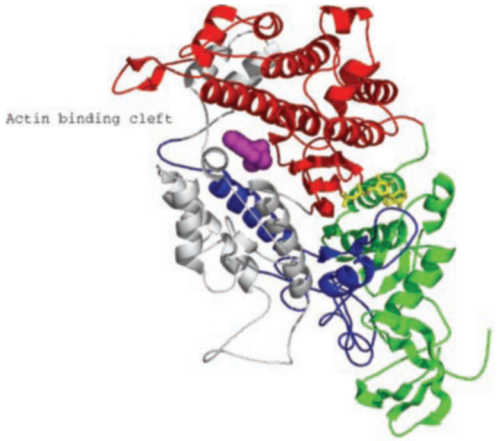

FIG. 7. **Proposed binding site of blebbistatin in myosin II.** The strongest conformer of the blebbistatin docking pattern in the structure of the *Dictyostelium* myosin II motor domain·ADP·AlF_4 complex (closed conformation) is shown (30). This blebbistatin conformer is positioned in the aqueous cavity located between the actin binding cleft and the switch I/switch II region. Blebbistatin binds to the open form of the myosin head at a similar location, but the binding is three times weaker. The two enantiomers of blebbistatin showed very similar binding patterns and binding energies. *Green*, 25-kDa domain; *red*, upper 50-kDa domain; *white*, lower 50-kDa domain, *blue*, 20-kDa domain; *yellow*, ADP; *magenta*, (*R*)-blebbistatin. Figure was prepared using the PyMOL Molecular Graphics System software (DeLano Scientific, San Carlos, CA).

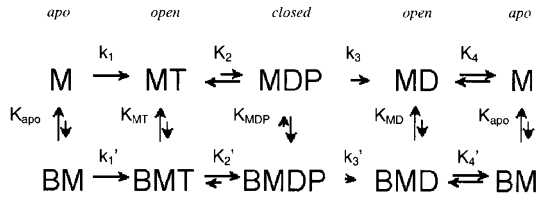

SCHEME 1. The symbols used are as follows: *B*, blebbistatin; *D*, ADP; *M*, myosin subfragment-1; *P*, phosphate; *T*, ATP. Equilibrium constants are expressed as proceeding from *left to right/bottom to top* in this scheme.

blebbistatin. On this basis, it was possible to distinguish functional and nonfunctional binding sites. Nonoverlapping regions of the binding patterns of skeletal muscle myosin and *Dictyostelium* myosin II were excluded. Consecutively, the overlapping parts of the binding patterns of *Dictyostelium* myosin II and those of noninhibited myosins were excluded as possible inhibitory binding sites. The remaining conformers of the binding pattern were located within the aqueous cavity between the actin binding cleft and the nucleotide-binding pocket (Fig. 7). It was concluded that this region was a possible inhibitory binding site of blebbistatin.

The above binding position exists both in the so-called open (MgATP complex) and closed ($MgAlF_4$ complex) states of *Dictyostelium* myosin II. The binding conformer of blebbistatin in the aqueous cavity of the closed state (Fig. 7) has the strongest interaction with the protein among the 100 docked ligands. Based on the calculated affinities, blebbistatin binding to this site is three times stronger to the closed state than to the open conformation. Comparison of the binding patterns of the (*R*)-(+)- and (*S*)-(−)-enantiomers of blebbistatin showed no significant difference in the case of all studied myosins.

DISCUSSION

Based on the results of the kinetic analysis, we propose a mechanism for blebbistatin inhibition of basal ATPase activity of S1 as depicted in Scheme 1. Blebbistatin binds relatively weakly to apoS1 (K_{apo} = 25 μM) and does not interfere with the nucleotide binding process. It has been shown that upon ADP binding, S1 adopts a conformation that is called the open state based on the position of the switch II loop in the active site of S1 (10). Because blebbistatin does not alter the ADP affinity of S1 ($K_4 = K'_4$ = 1.4 μM, Fig. 3*C*), it follows that the open state M·ADP complex has practically the same affinity for blebbistatin as apoS1 (K_{MD} = 24 μM, Scheme 1). The affinity of blebbistatin for both apoS1 and nucleotide-bound S1 in the open conformation is much lower than the steady-state $K_{½}$ value and the apparent affinity of blebbistatin for S1 during ATP hydrolysis (1–3 μM, Figs. 1*A* and 2*B*; Table I). Thus, it can be inferred that blebbistatin binds preferentially to a different nucleotide-bound S1 conformation. It has been shown that upon ATP binding, an open state M·ATP complex will initially be formed (10) that isomerizes into the closed state in which ATP hydrolysis takes place (10, 22, 29, 30). If blebbistatin binds ~10 times stronger to the closed M·ADP·P_i state than to the open conformation M·ATP complex, then it follows from thermodynamic considerations that the apparent equilibrium constant of ATP hydrolysis will be ~10 times elevated by the inhibitor. Indeed, this was seen in the quenched-flow experiments of Fig. 4 (K_2 = 0.35, K'_2 = 4). Thus, as K_{MDP} (Scheme 1) is about 3 μM (Fig. 2*B*), the open state M·ATP will bind blebbistatin with a K_{MT} of 35 μM, a value similar to that in the case of the M·ADP complex. Opening of switch II is kinetically coupled to the release of

phosphate (10, 22, 29). Thus, the stabilization of the closed state by blebbistatin will be accompanied by an inhibition of phosphate release (possibly through an effect on the preceding closed-open transition), the step that is rate-limiting in the ATPase cycle even in the absence of the inhibitor. In this respect, the inhibitory mechanism of blebbistatin is similar to that of *N*-benzyl-*p*-toluenesulfonamide, a specific inhibitor of fast skeletal myosin II (31). Blebbistatin slows down the steady-state ATPase rate of S1 from 0.08 s^{-1} to about 0.005 s^{-1}. The maximally inhibited rate will thus be determined by the decomposition of the quaternary blebbistatin·M·ADP·P_i complex (Scheme 1) either in the direction of phosphate release (k'_3) or blebbistatin dissociation from M·ADP·P_i (k_{MDP}).

Massive inhibition of the actin-activated ATPase by blebbistatin parallels that of the basal activity, leaving the extent of maximal actin-activation not greatly affected (~300-fold without blebbistatin, and ~100-fold in its presence). The K_{ATPase} value is not greatly changed by the inhibitor, implying that weak actomyosin interaction is not influenced by blebbistatin. Acto-S1 rigor binding and ATP-induced acto-S1 dissociation are not affected by the presence of 50 μM blebbistatin, probably because of the very low blebbistatin affinity of acto-S1. Thus, the communication between ATP- and actin-binding sites and the coupling between the bindings of these two ligands were not abolished.

Our results also bear a number of structural implications. Blebbistatin does not inhibit binding of any nucleotide ligands to apoS1, but it has markedly differing affinities for different S1 states and seems to favor intermediates in the closed conformation. Blebbistatin has no effect on several unconventional myosins (9), although the sequence of the structural elements comprising the ATP-binding site is highly conserved throughout the myosin superfamily (2). Thus, it is likely that the inhibitor does not directly bind into the nucleotide pocket of myosin II but causes specific perturbations in the structure of that region. Furthermore, blebbistatin and actin binding to S1 seem strongly antagonistic (Fig. 6*C*). All of these findings are in line with the computational docking results suggesting that the productive blebbistatin-binding site is within the aqueous cavity near the bottom of the actin binding cleft, and also close to the γ-phosphate-binding site. This binding site may be accessible to some extent even in the apo and open states of S1, but adoption of the switch II closed conformation may stabilize a more open state of the actin cleft and/or provide more favorable protein-ligand interactions, resulting in an increased blebbistatin affinity. Simulations indicate that blebbistatin binding in the cavity is three times stronger in the switch II closed state than in the open state, which is in reasonable agreement with the experimental binding data (K_d = 3 μM for closed state and 25–30 μM for open state, see Table I). The binding site is inaccessible in atomic structures of myosin isoforms that are not inhibited by blebbistatin (smooth muscle myosin and myosin V (9)).

In conclusion, blebbistatin can mostly be classified as uncompetitive based on the classical types of enzyme inhibitors; because it binds to a nucleotide-bound enzyme intermediate with highest affinity, it does not compete with substrate for binding sites on the enzyme, and it drastically lowers the V_{max} value. Blebbistatin blocks myosin II in an actin-detached state. Thus, it is a "benign" inhibitor conferring the great advantage that it does not cause adverse effects arising from rigid actomyosin cross-linking in cell biological applications. These features, together with its isoform specificity, make blebbistatin a useful compound in the investigation of all aspects of myosin II motor activity.

Acknowledgments—We thank Drs. Aaron F. Straight and Timothy J. Mitchison for providing blebbistatin; Estelle V. Harvey, Yue Zhang, and Antoine F. Smith for expert technical assistance; Dr. Howard D. White for comments on the manuscript; and Drs. Robert S. Adelstein and Earl Homsher for discussions.

REFERENCES

1. Brown, J. & Bridgman, P. C. (2003) *J. Histochem. Cytochem.* **51,** 421–428
2. Sellers, J. R. (1999) *Myosins,* Oxford University Press, New York
3. Yumura, S. & Uyeda, T. Q. (2003) *Int. Rev. Cytol.* **224,** 173–225
4. Wylie, S. R., Wu, P. J., Patel, H. & Chantler, P. D. (1998) *Proc. Natl. Acad. Sci. U. S. A.* **95,** 12967–12972
5. Wylie, S. R. & Chantler, P. D. (2001) *Nat. Cell Biol.* **3,** 88–92
6. Wylie, S. R. & Chantler, P. D. (2003) *Mol. Biol. Cell* **14,** 4654–4666
7. Ostap, E. M. (2002) *J. Muscle Res. Cell Motil.* **23,** 305–308
8. Straight, A. F., Cheung, A., Limouze, J., Chen, I., Westwood, N. J., Sellers, J. R. & Mitchison, T. J. (2003) *Science* **299,** 1743–1747
9. Limouze, J., Straight, A. F., Mitchison, T. J. & Sellers, J. R. (2004) *J. Muscle Res. Cell Motil.,* in press
10. Geeves, M. A. & Holmes, K. C. (1999) *Annu. Rev. Biochem.* **68,** 687–728
11. Margossian, S. S. & Lowey, S. (1982) *Methods Enzymol.* **85,** 55–71
12. Okamoto, Y. & Sekine, T. (1985) *J. Biochem.* (*Tokyo*) **98,** 1143–1145
13. Spudich, J. A. & Watt, S. (1971) *J. Biol. Chem.* **246,** 4866–4871
14. Cooper, J. A., Walker, S. B. & Pollard, T. D. (1983) *J. Muscle Res. Cell Motil.* **4,** 253–262
15. Wang, F., Kovacs, M., Hu, A., Limouze, J., Harvey, E. V. & Sellers, J. R. (2003) *J. Biol. Chem.* **278,** 27439–27448
16. Hetenyi, C. & van der Spoel, D. (2002) *Protein Sci.* **11,** 1729–1737
17. Morris, G. M., Goodsell, D. S., Halliday, R. S., Huey, R., Hart, W. E., Belew, R. K. & Olson, A. J. (1998) *J. Comput. Chem.* **19,** 1639–1662
18. Bagshaw, C. R., Eccleston, J. F., Eckstein, F., Goody, R. S., Gutfreund, H. & Trentham, D. R. (1974) *Biochem. J.* **141,** 351–364
19. Bagshaw, C. R. & Trentham, D. R. (1974) *Biochem. J.* **141,** 331–349
20. Batra, R. & Manstein, D. J. (1999) *Biol. Chem.* **380,** 1017–1023
21. Malnasi-Csizmadia, A., Woolley, R. J. & Bagshaw, C. R. (2000) *Biochemistry* **39,** 16135–16146
22. Malnasi-Csizmadia, A., Pearson, D. S., Kovacs, M., Woolley, R. J., Geeves, M. A. & Bagshaw, C. R. (2001) *Biochemistry* **40,** 12727–12737
23. Onishi, H., Konishi, K., Fujiwara, K., Hayakawa, K., Tanokura, M., Martinez, H. M. & Morales, M. F. (2000) *Proc. Natl. Acad. Sci. U. S. A.* **97,** 11203–11208
24. Park, S. & Burghardt, T. P. (2000) *Biochemistry* **39,** 11732–11741
25. Trybus, K. M. & Taylor, E. W. (1982) *Biochemistry* **21,** 1284–1294
26. Yengo, C. M., Chrin, L. R., Rovner, A. S. & Berger, C. L. (2000) *J. Biol. Chem.* **275,** 25481–25487
27. Bagshaw, C. R. & Trentham, D. R. (1973) *Biochem. J.* **133,** 323–328
28. Kurzawa, S. E. & Geeves, M. A. (1996) *J. Muscle Res. Cell Motil.* **17,** 669–676
29. Urbanke, C. & Wray, J. (2001) *Biochem. J.* **358,** 165–173
30. Fisher, A. J., Smith, C. A., Thoden, J. B., Smith, R., Sutoh, K., Holden, H. M. & Rayment, I. (1995) *Biochemistry* **34,** 8960–8972
31. Shaw, M. A., Ostap, E. M. & Goldman, Y. E. (2003) *Biochemistry* **42,** 6128–6135